Dynamical properties of the self-trapped exciton in AgCl as studied by time-resolved EPR at 95 GHz

O. G. Poluektov
Huygens Laboratory, Leiden University, P.O. Box 9504, 2300 RA Leiden, The Netherlands

M. C. J. M. Donckers
IBM Almaden Research Center, San Jose, California 95120-6099

P. G. Baranov
A.F. Ioffe Physico-Technical Institute, Polytechnischeskaya 26, 194021 St. Petersburg, Russia

J. Schmidt
Huygens Laboratory, Leiden University, P.O. Box 9504, 2300 RA Leiden, The Netherlands
(Received 21 September 1992; revised manuscript received 28 December 1992)

A study is made of self-trapped excitons in AgCl using cw and pulsed EPR techniques at 95 GHz. This type of spectroscopy, owing to its superior resolution and its time-resolved character, allows us to obtain detailed information about the properties of these excitons. The singlet-triplet splitting is determined with great accuracy and the result confirms that the exchange interaction, present between the electron and the hole making up the exciton, is very small. From a measurement of the dynamic properties of the exciton in the triplet state it appears that a tunneling process takes place between the different Jahn-Teller distorted configurations of the $(AgCl_6)^{4-}$ complex at a rate of 10^5 s^{-1} at temperatures as low as 1.2 K.

I. INTRODUCTION

The luminescent properties of AgCl have attracted considerable attention in the past two decades.[1-5] Part of this luminescence originates from the recombination of bound electron-hole pairs or excitons that are created in the crystal upon ultraviolet excitation. The hole is trapped in the $4d$ orbital of Ag^+, leading to the production of Ag^{2+}. In an octahedral crystal environment, the ^2D ground state of Ag^{2+} ($4d^9$) splits into an orbital doublet (E_g) and an orbital triplet (T_{2g}) with the doublet lying lower. The twofold degeneracy of the doublet state is lifted by a tetragonal Jahn-Teller distortion of the Ag coordination sphere resulting in a $d_{x^2-y^2}$-type ground state. Although this so-called self-trapped hole (STH) is largely localized at the Ag^+ ion, its wave function also contains contributions from the $3s$ and $3p$ orbitals of the neighboring Cl^- ions in the xy plane. The resulting $(AgCl_6)^{4-}$ complex can bind an electron in an extended s-orbital, thus forming the so-called self-trapped exciton (STE).

The properties of the excited states of this STE have been the subject of many investigations[6-14] using the method of optical detection of magnetic resonance (ODMR). However, several questions remained unclear, such as the dynamical properties of the excited singlet and triplet states, their exchange splitting, the ordering of the triplet sublevels, and the hyperfine interaction with the Ag and Cl nuclei. These problems cannot be solved with ODMR techniques at conventional microwave frequencies, because many resonance lines overlap (or partly overlap), and further because it is difficult to extract the dynamical properties from cw ODMR spectra.

In a previous paper we demonstrated the high spectral resolution that can be achieved when performing ODMR experiments at 95 GHz.[15] At this high frequency, the ODMR lines of the STE are well separated from those of the other paramagnetic centers occurring in the AgCl crystal. In particular, it proved possible to measure the effect of the magnetic-field-induced mixing, between the excited singlet state S_1 and the $|0\rangle$ sublevel of the triplet state T_0, on the positions of the ODMR transitions. From an analysis of the orientational dependence of the ODMR spectra, the exchange splitting $J=5\pm1$ cm^{-1} was obtained, in good agreement with previous estimates.[11] Here we will show that the same analysis allows us to establish unambiguously that the sign of the zero-field splitting parameter D is negative, in agreement with the conclusions of Yoshioka and Yamaga.[16] This result confirms that the zero-field splitting is dominated by contributions of second-order spin-orbit coupling and that spin-spin interactions are negligible.

This paper is concerned mainly with the results of an investigation of the dynamical properties of the excited singlet and triplet state of the STE. For this purpose, we have used electron-spin-echo (ESE) techniques in combination with pulsed laser excitation. The populating, depopulating, and spin-lattice relaxation processes have been studied and we conclude that a tunneling process takes place between the three different Jahn-Teller distorted configurations of the STE at temperatures as low as 1.2 K. In addition, we present results of ODMR experiments in magnetic field as well as in zero field which

 ©1993 The American Physical Society

further support the conclusions from the ESE experiments.

II. EXPERIMENT

In the ODMR experiments, the AgCl crystal was excited by a 100-W Hg arc in combination with a $NiSO_4/CoSO_4$ solution filter and an optical low-pass filter. The total luminescence was collected via a 375-nm optical high-pass filter and focused on a photomultiplier. In the ESE experiments at 95 GHz and in the microwave-induced delayed phosphorescence (MIDP) experiments in zero field, the excitation was provided by a pulsed XeCl excimer laser (pulse length 10 ns) at a wavelength of 308 nm.

The 95-GHz ODMR/ESE spectrometer used for the study of the STE in AgCl has been described in detail elsewhere.[17] Here we discuss only the aspects relevant to the results presented in this paper. For the ODMR experiments, the microwaves are generated by a Gunn diode operating at 94.9 GHz, amplitude modulated by a *p-i-n* diode at a frequency of about 70 Hz and guided to a Fabry-Pérot cavity. The advantage of this resonator is its open structure, that allows for easy optical access for excitation and detection. The quality factor Q is about 2000, and with the maximum microwave power of about 20 mW incident on the cavity the maximum microwave field B_1 is 3×10^{-5} T. The sample, with a typical dimension of $0.5\times0.5\times1.0$ mm^3, is placed in a quartz tube (outside diameter 1 mm). This quartz tube is carefully positioned in the center of the Fabry-Pérot resonator and can be rotated about a horizontal axis. The whole assembly, consisting of the cavity plus sample tube, is immersed in liquid helium in a cryostat with optical access. The static magnetic field $\mathbf{B}_0$ is provided by a split-coil superconducting magnet in a separate cryostat. This magnetic field can be rotated about a vertical axis. In combination with the rotation of the sample about the horizontal axis, this allows for orientation of the magnetic field along any desired direction of the crystal.

For the ESE experiments at 95 GHz, the microwaves were supplied by a phase-locked oscillator and shaped into short (20–50-ns) pulses by a combination of a pulsed amplifier and three *p-i-n* switches. Here, instead of the Fabry-Pérot resonator, we used a cylindrical cavity with slots in the bottom providing for the optical access. The great advantage of this cavity is its small volume, which results in a high concentration of the microwave power and high filling factor. With the same microwave power of 20 mW, the maximum microwave magnetic field B_1 is about ten times larger than in the Fabry-Pérot resonator. Typical values for the durations of the $\pi/2-$ and $\pi-$ pulses are 30 and 60 ns, respectively.

In the cw ODMR and MIDP experiments in zero field, the sample was placed in a tunable reentrant cavity of the type described by Erickson.[18] The microwaves were supplied by a backward wave oscillator and amplified to a power of about 1 W with a solid-state power amplifier. The microwaves were shaped into pulses with a duration between 2 and 5 μs by a *p-i-n*-diode switch.

For the MIDP experiments at temperatures below 1.2 K (the lowest temperature that can be achieved by us using liquid ^{4}He), a special ^{3}He cryostat was used that was immersed in the liquid-^{4}He bath. By reducing the pressure above the liquid ^{3}He, a temperature of 0.35 K can be reached.[19]

III. RESULTS

A. ODMR experiments at 95 GHz

In a previous paper,[15] we demonstrated how the exchange splitting J was derived, indirectly, via an analysis of the resonance fields of the ODMR transitions by taking into account the magnetic-field-induced mixing between the singlet state and the $|0\rangle$ sublevel of the triplet state T_0. This effect offers the possibility of a direct spectroscopic determination of the S_1-T_0 splitting, because S_1 carries some $|0\rangle$ character which makes the transition between the $|+1\rangle$ triplet sublevel and S_1 slightly allowed. Indeed, a careful search revealed a resonance line in the ODMR spectrum which we attribute to this transition, as can be seen in Fig. 1. From its position, we calculate $J=-5.37\pm0.01$ cm^{-1}. We also observe a weak line which we attribute to the "$\Delta m=2$" transition.

B. Electron-spin-echo experiments at 95 GHz

In Fig. 2, we present the ESE-detected EPR spectrum of the AgCl crystal at 94.9 GHz with $\mathbf{B}\|[001]$. The crys-

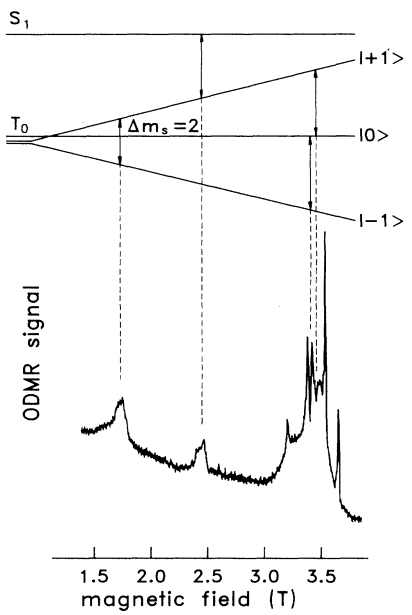

FIG. 1. The ODMR spectrum observed in the total luminescence of the AgCl crystal upon uv irradiation with a 100-W high-pressure Hg arc, and obtained by sweeping the magnetic field over a broad range. At 2.41 T, and ODMR line is visible which corresponds to the "forbidden" transition between the S_1 state and the $|+1\rangle$ sublevel of the triplet state of the STE. In addition, a line is visible which is assigned to the "$\Delta m_s=2$" transition. The microwaves at 94.9 GHz were amplitude modulated at 70 Hz and the detection took place synchronously in the emission intensity. The magnetic field is parallel to the crystal [100] axis. $T=1.2$ K.

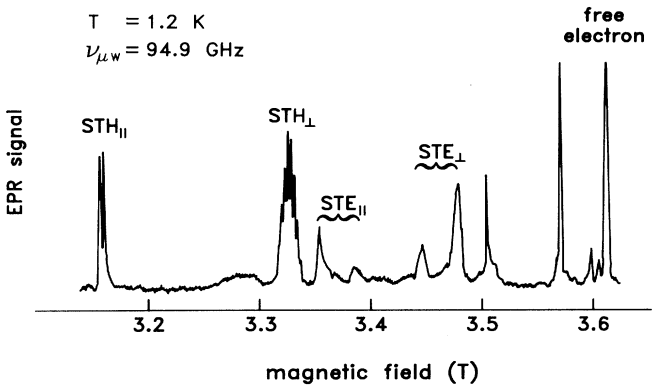

FIG. 2. The ESE-detected, field-swept, EPR spectrum of the AgCl crystal at 94.9 GHz with $\mathbf{B}\|[001]$ upon excitation by a laser flash at 308 nm (duration 10 ns). The $(\pi/2)-\tau-\pi$ microwave pulse sequence starts at a time t_d after the flash. The $(\pi/2)-$ and $\pi-$ pulse lengths are 30 and 60 ns, respectively, $\tau=4$ μs, and $t_d=5$ ms. $T=1.2$ K.

tal is first excited by a laser flash of the XeCl excimer laser at 308 nm and then subjected to a $(\pi/2)-\tau-\pi$ microwave pulse sequence starting at a time t_d after the laser flash. The spectrum is obtained by monitoring the echo height at a fixed value of t_d and τ and by sweeping the magnetic field. We recognize two signals of the STH, four of the STE, and one of the "free" electron.

In the discussion, we will concentrate on the signals of the STE. The two lines at 3.3541 and 3.3865 T correspond to the low-field and high-field transitions of the STE with $\mathbf{B}_0$ parallel to the distortion axis **z**: they are characterized by a g-value $g_{\|}^{\mathrm{STE}}=2.014$.[10,13] The two lines at 3.4460 and 3.4782 T are the low-field and high-field transitions of the other two sites of the STE with $\mathbf{B}_0\|\mathbf{x},\mathbf{y}$: they are characterized by a g value $g_{\perp}^{\mathrm{STE}}=1.960$.[10,13] The transitions at 3.1572 and 3.3250 T correspond to resonances of the STH, with B_0 parallel to the distortion axis **z** and $\mathbf{B}\|\mathbf{x},\mathbf{y}$ to g values $g_{\|}^{h}=2.147$ and $g_{\perp}^{h}=2.040$, respectively. The resonance of the "free" electron at 3.6061 T has an isotropic g value $g^{e}=1.881$.

We note that in the spectrum of Fig. 2 two new signals can be seen at 3.5016 and 3.5682 T, which exhibit the same orientational dependence as the STH but with $g_{\|}=1.937$ and $g_{\perp}=1.901$. We suggest that they originate from an electron trapped on an unknown defect. The possibility that they are related to a donor bound exciton, as observed in AgBr,[20] can be ruled out due to the fact that the signals do not disappear after shutting off the exciting light.

In our ESE study, we first measured the dephasing time T_2 of the signals in the spectrum displayed in Fig. 2. The results are listed in Table I. The remarkable finding is that the value of T_2 for the STE is about five times shorter than that for the STH and the FE. In addition, we estimated the spin-lattice relaxation time T_1 of all ground-state paramagnetic centers via the variation of the signal intensity with the repetition rate. These numbers are also given in Table I. We then measured the evolution of the spectrum of the STE by varying the delay time t_d after the laser flash. The result is shown in Fig. 3

TABLE I. The spin-spin relaxation time T_2 and the spin-lattice relaxation time T_1 of the various paramagnetic centers in the AgCl crystal at $T=1.2$ K. T_2 has been measured from the decay of the ESE signal as a function of 2τ. The value of T_1 has been estimated from the dependence of the ESE signal intensity as a function of the repetition rate of the ESE experiment.

	T_2 (μs) at 1.2 K	T_1 (ms) at 2.0 K	T_1 (ms)
STH$_{\|}$	110±5		10±2
STH$_{\perp}$	110+ 5		10±2
STE$_{\|}$	17.5±1.5	16.0±0.4	
STE$_{\perp}$	23.0±0.8	20.4±0.5	
$g_{\|}=1.937$	130±5		2±0.4
$g_{\perp}=1.901$	130±5		4±0.8
FE	90±5		10±2

for delay times varying from 0.003 to 80 ms. The striking aspect is that at the shorter delay time the signals, which are proportional to the population differences of the triplet sublevels connected by the microwave pulses, are zero. This means that within the experimental accuracy the populating rates of the sublevels are equal. The evolution of the signals is determined by the combined effect of decay and relaxation processes.

The evolution of the ESE signals of the four transitions in Fig. 3 either exhibit a two- or three-exponential behavior. For the high-field transition of the STE$_{\perp}$, the best fit is obtained with a three-exponential function. In contrast, the evolution of the STE$_{\perp}$ low-field transition can be fitted very well with a two-exponential function with two time constants which are equal, within the experimental error, to the two short-time constants derived for the STE$_{\perp}$ high-field transition. For the STE$_{\|}$ transitions a

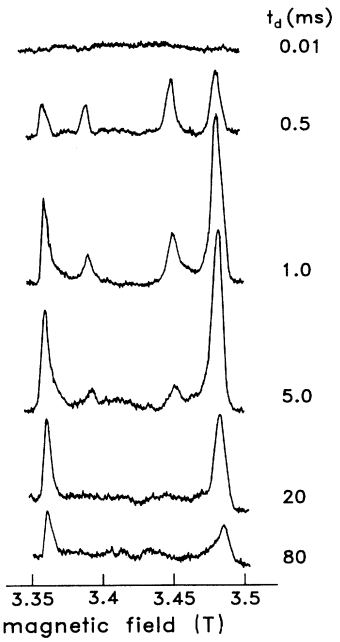

FIG. 3. The ESE-detected EPR spectrum of the STE as a function of the delay t_d after the laser flash.

similar behavior was found, but here the low-field transition was best fitted with a three-exponential and the high-field transition with a two-exponential curve. Again the two time constants derived from the two-exponential fit are equal, within the experimental error, to the two fast constants in the three-exponential fit.

The decay rates $k_1^{\parallel}, k_2^{\parallel}, k_3^{\parallel}$ and $k_1^{\perp}, k_2^{\perp}, k_3^{\perp}$, obtained from the fitting procedures of the low-field and high-field transitions, for the $STE_{\perp}$ and $STE_{\parallel}$ orientations have been plotted in Fig. 4 as a function of the temperature between 1.1 and 2.0 K. It is seen that the two fast components $k_1^{\perp}$ and $k_1^{\parallel}$ are equal, and independent of the temperature. The components $k_2^{\perp}$ and $k_2^{\parallel}$ are equal within the experimental accuracy but vary with the temperature. Further, we see that the two slow components $k_3^{\parallel}$ and $k_3^{\perp}$ differ and are also dependent on the temperature.

Before continuing with the result of the zero-field experiments, which complement the magnetic-field data, we will first give an interpretation of the observed decay rates in terms of the decay rates of, and the relaxation rate among, the sublevels of the triplet state of the STE. What happens is indicated schematically in Fig. 5. As mentioned already, the laser flash populates the sublevels equally, i.e., $P_+ = P_0 = P_-$ and the ESE signals, which measure the population differences, are initially zero. Then in the first 0.5 ms, the high-field and low-field signals of the $STE_{\parallel}$ and of the $STE_{\perp}$ start to develop equal absorptive intensities at a rate $k_1^{\parallel} = k_1^{\perp}$. This effect can only be understood by assuming that a dominant relaxation W_{+-} is present which transfers population from the $|+1\rangle$ to the $|-1\rangle$ sublevels. It is interesting to note that this rate W_{+-} is temperature independent, which is in agreement with the idea that the transfer from $|+1\rangle \rightarrow |-1\rangle$ corresponds to a direct process in which a phonon of energy $E(|+1\rangle) - E(|-1\rangle) \approx 190$ GHz is created. We come back to this point in the next section.

In the time interval between 1 and 5 ms we observe that the low-field signal of the $STE_{\parallel}$ and high-field signal of the $STE_{\perp}$ increase further but that the high-field signal of the $STE_{\parallel}$ and the low-field signal of the $STE_{\perp}$ decrease

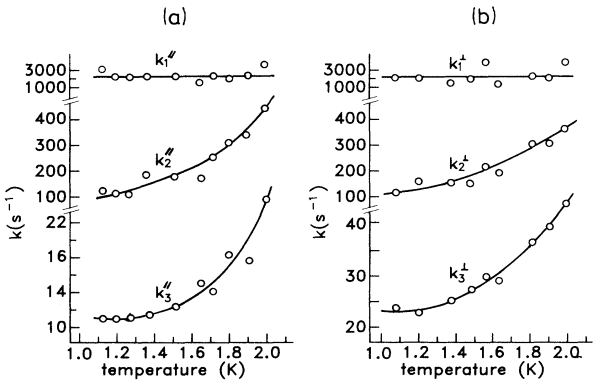

FIG. 4. The temperature dependence of the decay rates $k_1^{\parallel}, k_2^{\parallel}, k_3^{\parallel}$ and $k_1^{\perp}, k_2^{\perp}, k_3^{\perp}$ as derived from the evolution of the low-field and high-field transitions for the $STE_{\parallel}$ and $STE_{\perp}$ orientations.

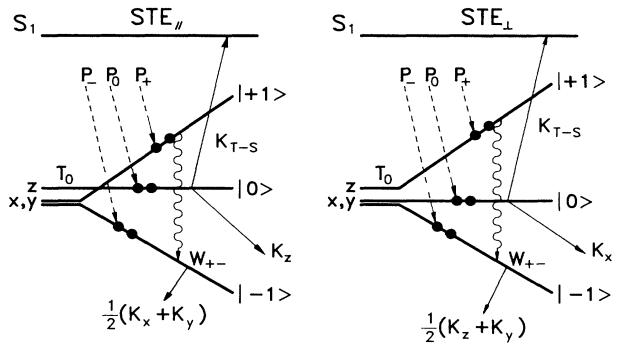

FIG. 5. A schematic diagram of the triplet state of the STE with the dynamic processes determining the populations of the sublevels. P_+, P_0, P_- are the relative populating rates, W_{+-} is the SLR relaxation rate from $|+1\rangle$ to the $|-1\rangle$ sublevel. k_{TS} is the thermally activated escape rate from $|0\rangle$ to S_1. k_z and k_x are the decay rates from $|0\rangle$ to S_0 for the parallel and perpendicular situations, respectively. $\frac{1}{2}(k_x + k_y)$ and $\frac{1}{2}(k_z + k_y)$ are the decay rates of the $|+1\rangle$ and $|-1\rangle$ sublevels with the magnetic field in the parallel or the perpendicular orientation, respectively.

to zero with rates $k_2^{\parallel} = k_2^{\perp}$ which depend on the temperature. In principle this effect can be explained by three processes. First, a thermally induced transfer k_{TS} from $|0\rangle$ to S_1 (S_1 carries $|0\rangle$ character due to the magnetic-field-induced mixing); second, a decay from $|0\rangle$ to the ground state S_0 (indicated by k_z for the $STE_{\parallel}$ and by k_x for $STE_{\perp}$); and third, a spin-lattice relaxation rate W_{0-} from $|0\rangle$ to $|-1\rangle$. A significant contribution of the intrinsic decay rates k_x, k_y, and k_z of the triplet sublevels to $k_2^{\parallel}$ or $k_2^{\perp}$ is improbable because k_x, k_y, and k_z are expected to be temperature independent. (Later we will see that k_x, k_y, and k_z are too small to contribute to $k_2^{\parallel}$ or $k_2^{\perp}$.) Further, we exclude the W_{0-} relaxation since it is expected to be temperature independent in analogy with the W_{+-} process. This leaves the k_{TS} process as the only candidate. Indeed the temperature dependence of $k_2^{\parallel}$ and $k_2^{\perp}$ can be fitted to an exponential curve with an activation energy of 3–5 cm^{-1}. This conclusion, however, has to be considered with care because of the limited temperature range and the uncertainty of the data.

In the time interval between 5 and 100 ms, only the low-field $STE_{\parallel}$ and high-field $STE_{\perp}$ signals have remained and start to decay with rates $k_3^{\parallel}$ and $k_3^{\perp}$, respectively. These rates become temperature independent below 1.3 K, as can be seen from Fig. 4, and reach the values $k_3^{\parallel} = 11 \pm 0.5\ s^{-1}$ and $k_3^{\perp} = 22 \pm 1\ s^{-1}$, respectively. We assume that at this temperature, the population in $|-1\rangle$ decays exclusively to S_0 and that relaxation to $|0\rangle$ or $|+1\rangle$ or escape to S_1 is negligible. Thus $k_3^{\parallel} = \frac{1}{2}(k_x + k_y) = 11 \pm 0.5\ s^{-1}$ and $k_3^{\perp} = \frac{1}{2}(k_z + k_y) = 22 \pm 1\ s^{-1}$ and we derive $k_x = k_y = 11 \pm 0.5\ s^{-1}$ and $k_z = 33 \pm 1.5\ s^{-1}$.

Thus from an analysis of the evolution of the ESE signals at 95 GHz after the laser flash we have obtained a rather complete picture of the dynamic processes determining the population distribution of the triplet sublevels. To confirm the conclusion about the decay rates k_x k_y and k_z, we have performed time-resolved ODMR ex-

periments in zero field, where we expect to be able to determine these rates directly.

C. ODMR and time-resolved ODMR in zero field

In Fig. 6, we present a recording of the T_0^z-$T_0^{x,y}$ transition obtained by scanning amplitude-modulated microwaves through resonance while detecting synchronously in the optical emission. The line is observed with a signal-to-noise ratio which is considerably better than the recording by Marchetti and Tinti,[10] and allows the observation of two components with a separation of 45±4 MHz. We attribute the dominant contribution to this splitting to the hyperfine (hf) interaction term $A_{zz}S_zI_z$ of the triplet spin with the Ag^{107} and Ag^{109} ($I=\frac{1}{2}$) nuclear spins. This term $A_{zz}S_zI_z$ gives matrix elements between T_0^x and T_0^y, but since these two levels are degenerate it will lead to a first-order splitting of these levels equal to A_{zz}.[21] The terms $A_{xx}S_xI_x$ and $A_{yy}S_yI_y$ of the Ag nuclei only give second-order shifts of the order of 2 MHz. Further, for the Cl nuclei the term $A_{zz}S_zI_z$ is zero and the terms $A_{xx}S_xI_x$, $A_{yy}S_yI_y$ also can give only second-order shifts of about 2 MHz. It is interesting to note that for the STH, a hyperfine interaction $A_{zz}=93\pm6$ MHz with the Ag-nuclear spins has been reported,[2] i.e., almost exactly twice the value observed by us for the STE. We come back to this point in the next section.

In the time-resolved ODMR experiments, we excite the sample again with the 308-nm flash of the XeCl laser and follow the subsequent decay of the phosphorescence. At a delay t_d, we create the microwave-induced delayed phosphorescence (MIDP) signal via a microwave pulse which connects T_0^z with $T_0^{x,y}$. In the absence of relaxation between the sublevels, the decay of this signal is given by:[22]

$$I_{\mathrm{MIDP}}(t-t_d)=F\{k_z^r\exp[-k_z(t-t_d)] - k_y^r\exp[-k_y(t-t_d)]\} . \quad (1)$$

Here F is a population transfer factor which depends on the intensity of the microwave field, among other things.

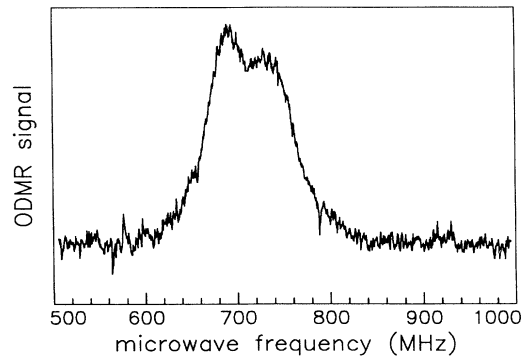

FIG. 6. The zero-field ODMR spectrum of the STE obtained by scanning amplitude-modulated microwaves through resonance while detecting synchronously in the optical emission. The modulation frequency is 43 Hz. $T=1.2$ K.

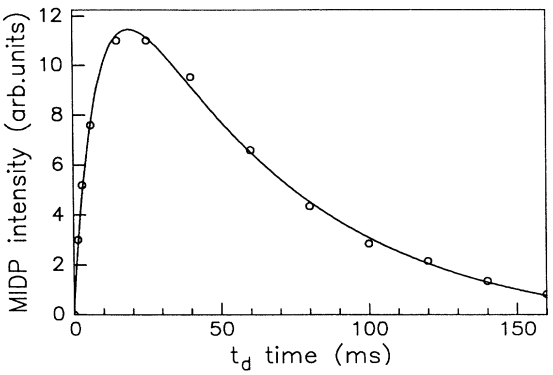

FIG. 7. A plot of the height I_{MIDP} of the MIDP signal as a function of t_d. The open circles represent the experimental data and the solid line is the result of a two-exponential fit with expression (2). The microwave frequency is 725 MHz. $T=1.2$ K.

The constants k_z^r and k_y^r are the radiative decay rates of T_0^z and T_0^y and k_z and k_y their total decay rates. Thus from fitting expression (1) to the shape of the MIDP signal, we obtain the ratio k_z^r/k_y^r ($=k_z^r/k_x^r$) and the decay rates k_z and k_y ($=k_x$).

The expression for the height of the MIDP signal as a function of t_d is given by[22]

$$I_{\mathrm{MIDP}}(t_d)=F\{N_z(0)\exp(-k_zt_d)-N_y(0)\exp(-k_yt_d)\} . \quad (2)$$

Thus, repeating the experiment and measuring this amplitude as a function of t_d (Fig. 7), we not only derive k_z and k_y ($=k_x$) but moreover the ratio of the populations $N_z(0)$: $N_y(0)$ ($=N_x(0)$). We find that $N_x(0)=N_y(0)=N_z(0)$ and thus that the populating rates of the three triplet sublevels in zero magnetic field are equal, just as in the presence of the magnetic field of 3.2 T.

In the actual experiment, in the MIDP signal we observe two time constants k^f and k^s which may contain a

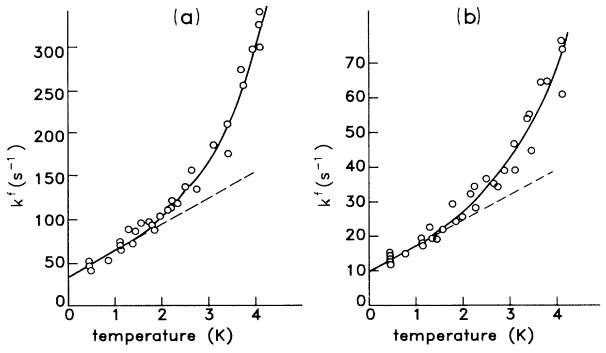

FIG. 8. The temperature dependence of (a) the "fast" component k^f and (b) the "slow" component k^s, as obtained from the fitting of the MIDP signals of the $T_0^z-T_0^{x,y}$ zero-field transition. The open circles represent the experimental data and the solid line is a fit to expression (3). The broken line indicates the part of expression (3) which depends linearly on T.

TABLE II. The time constants $k_0^{f,s}$, $k_1^{f,s}$, $k_2^{f,s}$ and the activation energy ΔE as defined by Eq. (3). The values are obtained from the fits of this equation to the experimental results shown in Fig. 8.

k_0^s (s^{-1})	k_0^f (s^{-1})	k_1^s ($s^{-1}K^{-1}$)	k_1^f ($s^{-1}K^{-1}$)	k_2^s (s^{-1})	k_2^f (s^{-1})	ΔE (cm^{-1})
(10±2)	(30±3)	(10±2)	(37±4)	(5±2)×10^2	(4.5±2)×10^3	(8±4)

contribution of relaxation between the triplet sublevels. To check to what extent this relaxation contributes, we have measured k^f and k^s as functions of the temperature between 0.4 and 4.2 K. The results are presented in Figs. 8(a) and 8(b). The two curves have been fitted to the expression

$$k^{f,s}=k_0^{f,s}+k_1^{f,s}T+k_2^{f,s}e^{-\Delta E/KT}, \quad (3)$$

as shown in Figs. 8(a) and 8(b). In Table II, we summarize the results for the various constants obtained from this fit.

We see that at $T=0$, K, the value of the "fast" and "slow" decay rates are equal (within the experimental accuracy) to the decay rates $k_z=33\pm1.5$ s^{-1} and $k_y=k_x=11\pm0.5$ s^{-1}, derived from the experiments in magnetic field. This convinces us that these values represent the intrinsic decay rates of the zero-field sublevels T_0^z and $T_0^{x,y}$ to the S_0 ground state. Moreover, we find that the ratio k_z^r/k_y^r $(=k_z^r/k_x^r)=3.0\pm0.1$. The next term in (3) in all probability represents a direct-process spin-lattice relaxation between the sublevels. This is reasonable because in the temperature range 0.42–2 K, the ratio $\hbar\omega/kT\ll1$ and a spin-lattice relaxation rate proportional to ω^2T are expected for a non-Kramers doublet such as our triplet state in zero field. Finally, the third term, with its exponential dependence on an activation energy of 8±4 cm^{-1}, is thought to represent the thermally induced escape from T_0 to S_1. In view of the limited temperature region over which the measurement has been performed, we cannot exclude the possibility that this part of the relaxation is caused by a Raman-like process.

IV. DISCUSSION

The experiments at 95 GHz have revealed various aspects of the STE in AgCl. As we have demonstrated already in our previous paper, the S_1-T_0 splitting can be derived from the effects of the magnetic-field-induced mixing between the $|0\rangle$ triplet sublevel and the singlet state S_1. Here we have shown that it is possible to determine J even more precisely via the direct observation of the "forbidden" transition between S_1 and the $|+1\rangle$ sublevel of T_0. The value of 5.37±0.01 cm^{-1} is in agreement with the estimate of 6–7 cm^{-1} of Yoshioka, Sugimoto, and Yamaga based on an analysis of the intensity of the ODMR transitions at K-band microwave frequencies. This exchange splitting is somewhat smaller than the values obtained for the STE's in alkali halides,[23] and somewhat larger than that of the free exciton in AgBr (2.5 cm^{-1}).[24] It confirms that the overlap of the orbitals of the STH and the electron is very small.

The zero-field splitting parameter D is found to be negative from the analysis of the position of the ODMR lines. This finding confirms the theoretical prediction of Yoshioka and Yamaga.[16] These authors showed that the contribution of second-order spin-orbit interaction to D dominates and that spin-spin interaction can be neglected. Further, we find from the zero-field ODMR experiments a hyperfine interaction term $A_{zz}^{STE}=45\pm4$ MHz. This value is almost exactly half that for the hf interaction of the STH with the Ag^{107} and Ag^{109} $I=\frac{1}{2}$ nuclear spins ($A_{zz}^{STH}=93\pm6$ MHz). When also attributing the term $A_{zz}^{STE}=(45\pm4)$ MHz to coupling with the Ag nuclear spins, we conclude that this hf interaction in the STE is dominated by the electron spin of the hole and that the contribution of the spin of the bound electron is small. Apparently the electron in the STE is very delocalized and the density of its wave function at the position of the Ag nucleus is at least two orders of magnitude smaller than would be expected on the basis of a 5s-like orbital.[25] The time-resolved ESE and ODMR experiments have allowed us to unravel the populating and decay processes of the triplet spin levels. First, we have found that the relative populating rates in zero field as well as in magnetic field are equal. Apparently, upon excitation over the band-gap, pairs of electrons and holes are formed and the probability of generating the singlet state or the three sublevels of the triplet state of the STE are equal. With regard to the decay process, we see that the rates $k_z:(k_y,k_x)=k_z^r:(k_y^r,k_x^r)=3:1$. This result can be understood by considering the spin-orbit coupling in the STE, which mixes singlet character into the triplet substates. To illustrate the pathways of spin-orbit coupling, in Fig. 9 we present a schematic diagram of the lower excited states of the STE.

The (simplified) level scheme of Fig. 9 has been derived by considering the STE as a STH with an electron loosely

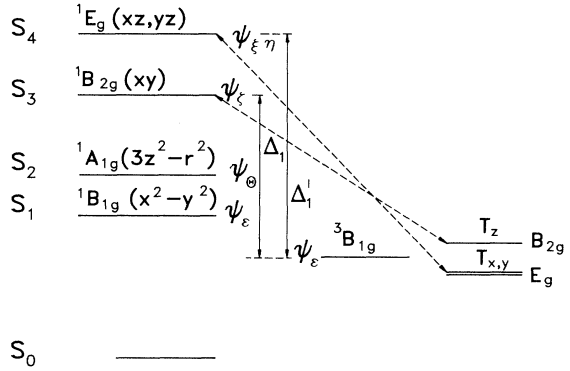

FIG. 9. A simplified energy-level scheme of the STE. The dashed lines indicate the routes of spin-orbit coupling between the lowest triplet state and the excited singlet states. At the right side of the triplet state we have indicated the total symmetry, which is the product of the orbital and spin symmetries.

bound to it. The molecular orbitals describing the STH are linear combinations of the Ag-4d orbitals and 3s and 3p orbitals of the six surrounding Cl ions. In an octahedral field with tetragonal distortion, the $\phi_\epsilon(d_{x^2-y^2})$ orbital involving the $d_{x^2-y^2}$ wave function of the Ag ion is lowest in energy. For our discussion, we also need to consider the $\phi_\zeta(d_{xy})$, $\phi_\xi(d_{yz})$, and $\phi_\eta(d_{xz})$ orbitals. The electron bound to the STH to form the STE is assumed to be in an s-like orbital. Neglecting the overlap integrals between the electron and hole wave functions, we find, for the wave functions describing the lowest B_{1g} singlet and triplet states of the STE,

$$^1\psi_\epsilon=\frac{1}{\sqrt{2}}\{\phi_\epsilon(\mathbf{r}_1)\phi_s(\mathbf{r}_2)+\phi_s(\mathbf{r}_1)\phi_\epsilon(\mathbf{r}_2)\}\sigma(1,2)\ , \tag{4}$$

$$^3\psi_\epsilon\frac{1}{\sqrt{2}}\{\phi_\epsilon(\mathbf{r}_1)\phi_s(\mathbf{r}_2)-\phi_s(\mathbf{r}_1)\phi_\epsilon(\mathbf{r}_2)\}\tau_i(1,2) \quad (i=x,y,z)\ , \tag{5}$$

$$\sigma(1,2)=\frac{1}{\sqrt{2}}\{\alpha(1)\beta(2)-\beta(1)\alpha(2)\}\ , \tag{6}$$

$$\tau_x(1,2)=\frac{1}{\sqrt{2}}\{\beta(1)\beta(2)-\alpha(1)\alpha(2)\}\ , \tag{7}$$

$$\tau_y(1,2)=\frac{i}{\sqrt{2}}\{\alpha(1)\alpha(2)+\beta(1)\beta(2)\}\ , \tag{8}$$

$$\tau_z(1,2)=\frac{1}{\sqrt{2}}\{\alpha(1)\beta(2)+\beta(1)\alpha(2)\}\ . \tag{9}$$

The spin-orbit coupling admixes small amounts of excited singlet and triplet states into $^3\psi_\epsilon$. Since this interaction is totally symmetric, we only have to consider the excited singlet states of symmetry species $^1B_{2g}$ and ^1E_g, which are related to excitations of the STH to $b_{2g}(\phi_\zeta(d_{xy}))$ and $e_g(\phi_\eta(d_{xz}))$ states. In these excited states, the electron is assumed to have the same wave function as in the lowest singlet and triplet states.

The wave functions of the lowest triplet state of the STE in our approximation become (we neglect admixture of excited triplet states)

$$^3\Psi_z=^3\psi_\epsilon\tau_z-\frac{i2\lambda_{\epsilon\zeta}}{2\Delta_1}{}^1\psi_\zeta\sigma\ , \tag{10}$$

$$^3\Psi_y=^3\psi_\epsilon\tau_y+\frac{\lambda_{\epsilon\eta}}{2\Delta_1'}{}^1\psi_\eta\sigma\ , \tag{11}$$

$$^3\Psi_x=^3\psi_\epsilon\tau_x+\frac{i\lambda_{\epsilon\xi}}{2\Delta_1'}{}^1\psi_\xi\sigma\ . \tag{12}$$

Here $\lambda_{\epsilon\zeta}$, $\lambda_{\epsilon\eta}$, and $\lambda_{\epsilon\xi}$ are the effective spin-orbit coupling constants between b_{1g} and b_{2g} orbitals and b_{1g} and e_g orbitals of the STH, respectively. Further, Δ_1 and Δ_1' are the energy separations between these orbitals.

To derive the relative radiative decay rates from the three triplet sublevels, we need to know the effective spin-orbit coupling constants. Fortunately, these have been estimated from an analysis of the g values of the STH (Ref. 16) to be

$$\lambda_{\epsilon\zeta}=-778\ \text{cm}^{-1}\ ,\quad \lambda_{\epsilon\xi}=\lambda_{\epsilon\eta}=914\ \text{cm}^{-1}\ .$$

Taking $\Delta_1\approx\Delta_1'$ and assuming that k_i $(i=x,y,z)$ is proportional to the square of the coefficient of the singlet admixture in $^3\psi_i$, we find that the rates of the radiative decay rates,

$$k_z^r:k_{y,x}^r\simeq 2.9:1\ ,$$

are in good agreement with the observed ratio of 3.0 ± 0.1 for the relative radiative and total decay rates of T_0^z and $T_0^{x,y}$. Here we mention that we have made the simplifying assumption that the radiative transition probabilities from the excited $^1B_{2g}$ and ^1E_g states, which are induced by odd-parity perturbing fields of lattice vibrations, are equal.

Finally, we discuss the spin-lattice relaxation. Here the remarkable observation is the presence of the dominant and temperature-independent relaxation rate W_{+-} from the $|+1\rangle$ to the $|-1\rangle$ magnetic sublevels. We propose that it is caused by a tunneling process in which the elongation of the $(AgCl_6)^{4-}$ complex changes direction from one cubic axis to another one. The consequence of this tunneling is that the expression for the zero-field Hamiltonian becomes time dependent and varies between $DS_z^2-\frac{1}{3}S(S+1)$, and $DS_x^2-\frac{1}{3}S(S+1)$ or $DS_y^2-\frac{1}{3}S(S+1)$. The two latter forms contain the bilinear operators S_x^2 and S_y^2, which are capable of inducing *selectively* transitions between the $|+1\rangle$ and $|-1\rangle$ sublevels.

In order to calculate the resulting relaxation rate W_{+-}, we assume that this relaxation is described by a direct process in which a single quantum is exchanged between the spin system and the phonon bath, i.e., the ratio of the rates W_{+-} and W_{-+} is given by the expression

$$\frac{W_{+-}}{W_{-+}}=\frac{A+B\rho_{\text{ph}}(\omega)}{B\rho_{\text{ph}}(\omega)}=\frac{1+\bar{p}}{\bar{p}}=\exp\frac{\Delta E}{kT}\ . \tag{13}$$

Here $\rho_{\text{ph}}(\omega)$ is the phonon energy density per unit frequency and A and B are the well-known Einstein coefficients for spontaneous emission and for stimulated emission and absorption, respectively. Further, $\rho_{\text{ph}}(\omega)$ is related to the phonon occupation number $\bar{p}$ via the relation $\rho_{\text{ph}}(\omega)=\Sigma\bar{p}\hbar\omega$, where the quantity Σ is the number of phonon modes per unit volume per unit frequency range.

In our case, $\bar{p}\ll 1$ and the decay W_{+-} is dominated by spontaneous emission, a process which cannot be accounted for by the semiclassical treatment of spin-lattice relaxation. This poses no problem because it suffices to calculate the rate for the induced transitions. The rate for spontaneous emission can then be derived from the Einstein relation between the coefficients A and B.

The standard formula for the induced transition probability applied to our case yields

$$W_{-+}=B\rho_{\text{ph}}(\omega)=\frac{2\pi}{\hbar^2}|\langle+1|DS_{x,y}^2(t)|-1\rangle|^2 f(\omega)\ , \tag{14}$$

where $f(\omega)$ is the line-shape function. When assuming that the time dependence of $DS_x^2(t)$ and $DS_y^2(t)$ is given by a random function fluctuating around an average value and is characterized by an autocorrelation function with a correlation time τ_c, we can calculate the mean-square fluctuations of the matrix element $\langle+1|DS_{x,y}^2(+)|-1\rangle$ at frequency ω_0 (the splitting fre-

quency of the two levels $|+1\rangle$ and $|-1\rangle$),

$$W_{-+}=B\rho_{\rm ph}(\omega)=\frac{1}{\hbar^2}|\langle+1|DS_{x,y}^2|-1\rangle|^2\frac{2\tau_c}{1+\omega_0^2\tau_c^2}\ . \tag{15}$$

The only unknown parameter here is the value of τ_c. For an estimate of τ_c, which in our model represents the transfer time of the tunneling process, we use the value of the triplet spin dephasing time T_2. The rationale is that the tunneling will interrupt the precession of the triplet spins and thus affect their dephasing rate.

Indeed, we see from Table I that T_2 for the STE is about five times shorter than for the STH and the free electron (FE). When using $\tau_c\approx10^{-5}$ s, we derive $W_{-+}=B\rho_{\rm ph}(\omega)\approx2\ {\rm s}^{-1}$ at 1.2 K, and via the Einstein relation we find $W_{+-}\simeq1.5\times10^3\ {\rm s}^{-1}$ for the spontaneous emission rate, in good agreement with the experimental finding of $2\times10^3\ {\rm s}^{-1}$.

It is interesting to see that the value of T_2 shortens between 1.2 and 2.0 K (see Table I). This indicates that the tunneling process is not a purely coherent process but that a thermally activated contribution is present. It would be interesting to measure the variation of T_2 over a wider temperature range to estimate the activation energy of this process. Further, we note that T_2 for the parallel orientation is somewhat shorter than for the perpendicular situation. This difference can be understood by the fact that in the parallel (z) orientation, energy jumps (to x or y) lead to a change in resonance frequency and thus to a dephasing of the triplet spins. In contrast in the perpendicular orientation, only half of the jumps (to z) destroy the phase coherence.

In zero field, we observe a spin-lattice relaxation rate which, at least in the temperature region between 0.4 and 2 K, exhibits a linear dependence of T, also characteristic of a direct process. The important differences with the magnetic-field case are twofold. First, we are now in the situation $\hbar\omega_0\ll kT$, and spontaneous emission is negligible. Second, the operator S_x^2 and S_y^2 in the matrix element of Eq. (15) does not connect the zero-field spin states. Hence it is not clear whether the same tunneling process is involved in the observed relaxation process and it is possible that the relaxation is caused by a direct contact with the phonon bath.

V. CONCLUSION

Electron paramagnetic resonance spectroscopy at 95 GHz has enabled us to derive detailed information about the properties of self-trapped excitons in AgCl. In particular, the electron-spin-echo technique, in combination with pulsed laser excitation, offers a number of advantages compared to cw ODMR at conventional frequencies. First of all, a signal-to-noise ratio can be achieved in the ESE-detected EPR spectrum that is much higher than at conventional frequencies. This is related to the fact that in a magnetic field of 3.4 T, a very favorable path of relaxation is present in the triplet state. Thus by choosing a proper delay time after the laser flash, a population difference of about 100% can be achieved between the triplet sublevels. Further, at the high magnetic field necessary for the experiment, the EPR spectrum of the STE is well separated from that of other paramagnetic species, owing to their differences in g value. As a result, we can observe the effect of the magnetic-field-induced S_1-T_0 mixing and deduce the splitting of these two levels. The result confirms that the overlap of the wave functions of the hole and the electron forming the STE is indeed very small. It is even possible to observe the transitions between the $|+1\rangle$ sublevel of T_0 and S_1 in the ODMR spectrum.

The time-resolved nature of the ESE technique enables us also to study the dynamic properties of the triplet state. One of the most remarkable findings is the very fast relaxation rate W_{+-} from the $|+1\rangle$ to the $|-1\rangle$ sublevels. This "$\Delta m=2$"-type of relaxation can be regarded as a spontaneous emission process. It can be understood on the basis of a tunneling between the three possible configurations of the Jahn-Teller distorted $(AgCl_6)^{4-}$ complex. By equating the value $T_2\simeq10^{-5}$ s, measured for the triplet spin dephasing time at 1.2 K, to the correlation time of this tunneling process, we derive a theoretical value for W_{+-} which is in very good agreement with the experimental observation. The result shows that the tunneling rate, and for instance its dependence on the temperature, can be found directly from a measurement of T_2.

It is interesting to note that Yamaga, Sugimoto, and Yoshioka[13] observed an isotropic line in the ODMR spectrum of the STE at 4.2 K, which they explained on the basis of tunneling between the different configurations of the $(AgCl_6)^{4-}$ complex. However, their interpretation would mean that, at this temperature, the rate of tunneling would be faster than $10^9\ {\rm s}^{-1}$, a value which is difficult to relate with our finding of $10^5\ {\rm s}^{-1}$ at 1.2 K. Nevertheless we agree with their suggestion that the presence of the bound electron in the STE apparently lowers the barrier height between the three configurations of the Jahn-Teller distorted complex compared with that in the STH.

A further result of the time-resolved ESE experiments is the value of the decay rates of the triplet sublevels to the ground state S_0. It appears that their ratio can be explained on the basis of the relative amount of singlet character mixed by spin-orbit into the triplet sublevels. We mention that the assignment of the observed decay of the $|0\rangle$ triplet sublevel to a thermal excitation to S_1 can also be seen as a manifestation of the magnetic-field-induced mixing between these two states.

ACKNOWLEDGMENTS

This work is part of the research program of the "Stichting voor Fundamenteel Onderzoek der Materie" (FOM), and has been made possible by the financial support from the "Nederlands Organisatie voor Wetenschappelijk Onderzoek" (NWO). The authors wish to thank Professor H. Bill for very stimulating discussions.

[1]G. C. Smith, Phys. Rev. A **140**, 221 (1965).
[2]C. L. Marquardt, R. T. Williams, and M. N. Kabler, Solid State Commun. **9**, 2285 (1971).
[3]H. Kanzaki and S. Sakuragi, Solid State Commun. **9**, 1667 (1971).
[4]H. Kanzaki, S. Sakuragi, and K. Sakamoto, Solid State Commun. **9**, 999 (1971).
[5]M. Yamaga, M. Fukui, and Y. Hayashi, J. Phys. Soc. Jpn. **38**, 1548 (1975).
[6]W. Hayes and I. B. Owen, J. Phys. C **9**, L69 (1976).
[7]K. Murayama, K. Morigaki, S. Sakuragi, and H. Kanzaki, J. Phys. Soc. Jpn. **41**, 1617 (1976).
[8]W. Hayes, I. B. Owen, and P. J. Walker, J. Phys. C **10**, 1751 (1977).
[9]W. Hayes and I. B. Owen, J. Phys. C **11**, L607 (1978).
[10]A. P. Marchetti and D. S. Tinti, Phys. Rev. B **24**, 7361 (1981).
[11]H. Yoshioka, N. Sugimoto, and M. Yamaga, J. Phys. Soc. Jpn. **54**, 3990 (1985).
[12]N. Sugimoto, H. Yoshioka, and M. Yamaga, J. Phys. Soc. Jpn. **54**, 4331 (1985).
[13]M. Yamaga, N. Sugimoto, and H. Yoshioka, J. Phys. Soc. Jpn. **54**, 4340 (1985).
[14]J. P. Spoonhower, F. J. Ahlers, R. S. Eachus, and W. G. McDugle, J. Phys. C **2**, 3021 (1990).
[15]M. C. J. M. Donckers, O. G. Poluektov, P. G. Baranov, and J. Schmidt, Phys. Rev. B **45**, 13 061 (1992).
[16]H. Yoshioka and M. Yamaga, J. Phys. Soc. Jpn. **54**, 841 (1985).
[17]R. T. Weber, J. A. J. M. Disselhorst, L. J. Prevo, J. Schmidt, and W. Th. Wenckebach, J. Magn. Reson. **81**, 129 (1989).
[18]L. E. Erickson, Phys. Rev. **143**, 295 (1966).
[19]J. F. C. van Kooten, M. G. Munowitz, J. Schmidt, and H. Benk, Mol. Phys. **52**. 1397 (1984).
[20]W. von der Osten and H. Stolz, J. Phys. Chem. Solids **51**, 765 (1990).
[21]J. Schmidt and J. H. van der Waals, Chem. Phys. Lett. **3**, 546 (1969).
[22]J. Schmidt and J. H. van der Waals, in *Time Domain Electron-Spin Resonance,* edited by L. Kevan and R. N. Schwartz (Wiley, New York, 1979), p. 343.
[23]P. J. Call, W. Hayes, R. Huzimura, and M. N. Kabler, J. Phys. C **8**, L56 (1975).
[24]M. Matsushita, J. Phys. Soc. Jpn. **35**, 1688 (1973).
[25]C. J. Delbecq, W. Hayes, M. C. O'Brien, and P. H. Yuster, Proc. R. Soc. London Ser. A **271**, 243 (1963).